

## Preparation of Monodisperse GeO<sub>2</sub> Nanocubes in a Reverse Micelle System

H. P. Wu,<sup>†</sup> J. F. Liu,<sup>†</sup> M. Y. Ge,<sup>†</sup> L. Niu,<sup>†</sup> Y. W. Zeng,<sup>†,‡</sup> Y. W. Wang,<sup>†,‡</sup> G. L. Lv,<sup>†,‡</sup>  
L. N. Wang,<sup>§</sup> G. Q. Zhang,<sup>†,§</sup> and J. Z. Jiang<sup>\*,†</sup>

Laboratory of New-Structured Materials, Department of Materials Science and Engineering, and  
Analysis and Testing Centre, Zhejiang University, Hangzhou, 310027, P. R. China, and  
Center for Analysis, Zhejiang Sci-Tech University, Hangzhou 310018, P. R. China

Received November 8, 2005. Revised Manuscript Received February 11, 2006

We report here a synthesis method for single-crystal monodisperse GeO<sub>2</sub> nanocubes in a reverse micelle system. Hydrolysis of germanium tetrachloride (GeCl<sub>4</sub>) in a micelle system produces GeO<sub>2</sub> nanocubes in the presence of oleylamine and cetyltrimethylammonium (CTAB). The average edge length of the cubes varies from 50 to 520 nm depending on the concentration of CTAB in the solution. The perfection and monodispersity of the nanocubes are greatly improved by decreasing the pH value of the water solution. Different morphologies such as capsules can be prepared by using octane as the oil phase. The BFDH and Hartman-Perdok methods were used to predict the morphology evolution during the growth of GeO<sub>2</sub> nanocubes.

### Introduction

Nanocrystals, consisting of small crystallites of diameter 1–500 nm, often have novel physical and chemical properties, differing from those of the corresponding bulk materials.<sup>1</sup> For example, nanometer-sized semiconductors have electronic and optical properties that depend on the particle size, making them potential candidates for applications where tunability of these properties is essential. The unique properties of nanocrystalline materials open up the general question of how crystallite size and shape affects the structural stability. The design of exotic nanoparticles (e.g., high-quality monodisperse nanometer-sized particles with desired shape and structure) has been investigated intensively in recent years<sup>2</sup> but still remains a challenge. Recently, much attention has been paid to the preparation of nanostructures of germanium dioxide (GeO<sub>2</sub>), including nanowhiskers,<sup>3</sup> nanowires,<sup>4</sup> nanorods,<sup>5</sup> nanosheets,<sup>6</sup> and nanofibers.<sup>7</sup> GeO<sub>2</sub> has many attractive properties: it is a dielectric oxide and a blue photoluminescence material with peak energies around 2.2 and 3.1 eV, and it has a refractive index and a linear

coefficient of thermal expansion that are higher than those for silicate (SiO<sub>2</sub>). Moreover, it is a promising material for optical waveguides and nanoconnections in optoelectronic communication and vacuum technology.<sup>8</sup> Here we report the preparation of monodisperse germanium dioxide in the form of single-crystal nanocubes with cube edges ranging from 50 to 520 nm, using a reverse micelle method. The origin of the formation of the nanocubes is investigated.

### Experimental Section

**Germanium Dioxide Nanocubes Synthesis.** To produce monodisperse GeO<sub>2</sub> nanocubes, germanium tetrachloride (GeCl<sub>4</sub>), heptane (or octane), and water were used as precursor, oil phase, and water phase, respectively. Oleylamine and cetyltrimethylammonium (CTAB) were used as surfactants. Two types of micelle solutions were prepared: (1) a 3 mL aqueous solution with pH = 1.0, 5 g of CTAB, and 9 mL of pentanol were added to 60 mL of heptane to form a transparent microemulsion; (2) 2 mL of a 0.5 M GeCl<sub>4</sub> tetrahydrofuran (THF) solution and 5 mL of oleylamine were added to 20 mL of heptane to form a transparent microemulsion. The GeCl<sub>4</sub> (THF)–oleylamine–oil phase solution was dropped into the water–CTAB–oil phase solution accompanied by strong magnetic stirring. The solution became turbid after 20 min, and the reaction was complete after 180 min. Subsequently, the particles were

\* Corresponding author. E-mail: jiangz@zju.edu.cn. Phone: +86 571 8795 2107. Fax: +86 571 8795 2107.

<sup>†</sup>Laboratory of New-Structured Materials, Department of Materials Science and Engineering, Zhejiang University.

<sup>‡</sup>Analysis and Testing Centre, Zhejiang University.

<sup>§</sup>Zhejiang Sci-Tech University.

- (1) (a) Hadjipanayis, G. C.; Siegel, R. W. *Nanophase Materials: Synthesis-Properties-Applications*; Kluwer Academic Publishers: Dordrecht, 1994. (b) Fiorani, D.; Sberveglieri, G. *Fundamental Properties of Nanostructured Materials*; World Scientific: Singapore, 1994. (c) Bruchez, M.; Moronne, J. M.; Gin, P.; Weiss, S.; Alivisatos, A. P. *Science* **1998**, *281*, 2013–2016. (d) Im, H. S.; Lee, Y. T.; Wiley, B.; Xia, Y. N. *Angew. Chem. Int. Ed.* **2005**, *44*, 2154–2157.
- (2) (a) Wang, X.; Zhuang, J.; Peng, Q.; Li, Y. *Nature*, **2005**, *437*, 121–124. (b) Park, J.; An, K.; Hwang, Y.; Park, J.; Noh, H.; Kim, J.; Park, J.; Hwang, N.; Hyeon, T. *Nat. Mater.* **2004**, *3*, 891–895. (c) Liu, Z.; Zhang, D.; Han, S.; Li, C.; Lei, B.; Lu, W.; Fang, J.; Zhou, C. *J. Am. Chem. Soc.* **2005**, *127*, 6–7. (d) Cao, M.; Hu, C.; Peng, G.; Qi, Y.; Wang, E. *J. Am. Chem. Soc.* **2003**, *125*, 4982–4983.
- (3) Tang, Y. H.; Zhang, Y. F.; Wang, N.; Bello, I.; Lee, C. S.; Lee, S. T. *Appl. Phys. Lett.* **1999**, *74*, 3824–3826.

- (4) (a) Bai, Z. G.; Yu, D. P.; Zhang, H. Z.; Ding, Y.; Wang, Y. P.; Gai, X. Z.; Hang, Q. L.; Xiong, G. C.; Feng, S. Q. *Chem. Phys. Lett.* **1999**, *303*, 311–314. (b) Wu, X. C.; Song, W. H.; Zhao, B.; Sun, Y. P.; Du, J. J. *Chem. Phys. Lett.* **2001**, *349*, 210–214. (c) Kalyanikutty, K. P.; Gundiah, G.; Govindaraj, A.; Rao, C. N. R. *J. Nanosci. Nanotechnol.* **2005**, *5*, 425–428.
- (5) (a) Zhang, Y. J.; Zhu, J.; Zhang, Q.; Yan, Y. J.; Wang, N. L.; Zhang, X. Z. *Chem. Phys. Lett.* **2000**, *317*, 504–509. (b) Hu, J. Q.; Li, Q.; Meng, X. M.; Lee, C. S.; Lee, S. T. *Adv. Mater.* **2002**, *14*, 1396–1399.
- (6) Adachi, M.; Nakagawa, K.; Sago, K.; Murata, Y.; Nishikawa, Y. *Chem. Commun.* **2005**, 2381–2383.
- (7) Viswanathamurthi, P.; Bhattarai, N.; Kim, H. Y.; Khil, M. S.; Lee, D. R.; Suh, E.-K. *J. Chem. Phys.* **2004**, *121*, 441–445.
- (8) (a) Saito, K.; Ikushima, A. J. *Appl. Phys. Lett.* **1997**, *70*, 3504. (b) Werner, M. J.; Fribery, S. R. *Phys. Rev. Lett.* **1997**, *79*, 4143.

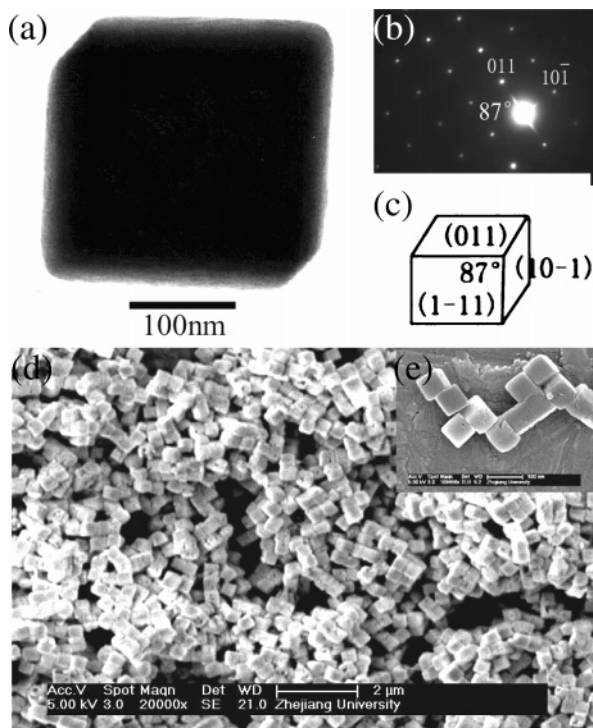


**Figure 1.** TEM and SEM images of  $\text{GeO}_2$  cubes prepared by the reverse micelle method using heptane as the oil phase and water solution of pH = 1.0. (a) TEM image of a single  $\text{GeO}_2$  cube. (b) SAED pattern of the particle in a; (c) illustration of the cubelike shape of the single crystal in a; (d) and (e) SEM images at different magnifications. Scale bar in e is 500 nm.

separated from the solution by centrifugation at  $10^4$  rpm for 20 min. The particles were then redispersed in ethanol in an ultrasonic bath. The centrifugation was repeated twice so as to remove all of the surfactant. In the final product, the precipitant containing nanocubes with white color was collected and redispersed in a small amount of xylene for further characterization.  $\text{GeO}_2$  samples with different shapes can be synthesized using water solutions of pH = 1.0, 3.0, 5.0, 7.0, 9.0, and 13.0.  $\text{GeO}_2$  nanocapsules can be formed when the pH of the water solution is 3.5–7.0 and heptane is replaced by octane.

**Characterization.** X-ray powder diffraction (XRD) was performed with a Rigaku D/MAX-2550PC powder X-ray diffractometer in Bragg–Brentano geometry, using  $\text{Cu K}\alpha$  radiation. The diffraction pattern was collected in the  $2\theta$  range 15–90° in steps of 0.02° and counting time 2 s/step. The crystallite size was calculated from the broadening of the diffraction peak at  $2\theta = 26^\circ$  using the Scherrer equation. Nanocrystal size, shape, and crystallography were characterized by transmission electron microscopy (TEM) using a JEOL TEM CX200 microscope operated at 160 kV. TEM samples were prepared by dropping the liquid containing  $\text{GeO}_2$  nanoparticles on a carbon-coated copper substrate. Field emission scanning electron microscopy (FESEM) was performed at FEI SIRION with specimens being coated with gold to improve the contrast.

## Results and Discussion

Figure 1 shows TEM and FESEM images of typical  $\text{GeO}_2$  nanocubes. A total number of 300 particles were observed and almost all of them are regular cubes with a mean edge length of 250–270 nm. Figure 1b shows a selected-area electron-diffraction (SAED) pattern of the single  $\text{GeO}_2$  cube in Figure 1c. The main diffraction spot is attributed to the  $(1\bar{1}1)$  plane. The two nearest diffraction spots correspond to

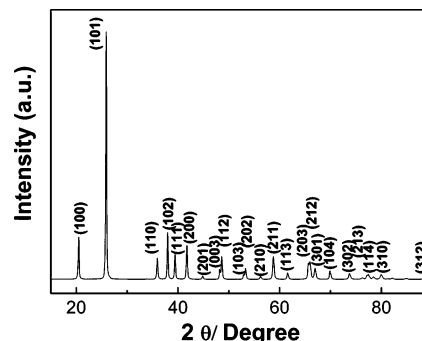


**Figure 2.** XRD pattern of nanocubes of hexagonal  $\text{GeO}_2$ .

$(011)$  and  $(10\bar{1})$ , respectively. The angle between the latter two planes is  $87^\circ$ . Thus, the  $\text{GeO}_2$  nanoparticles are not exactly cubic, but rather cubelike. For simplicity, we are using the term nanocubes. From FESEM images (Figures 1d and 1e) it is clear that the particles have a cubelike shape. Some cubes have small holes on the surface, possibly due to defects introduced during the growth of single crystals. Figure 2 shows an XRD pattern of a nanocrystalline  $\text{GeO}_2$  material produced by  $\text{GeCl}_4$  hydrolysis with a pH = 1.0 water solution. All diffraction peaks can be indexed according to a pure hexagonal phase [space group:  $P3_112$ ] ( $\alpha\text{-GeO}_2$ ) with lattice constants  $a = 4.993 \text{ \AA}$  and  $c = 5.661 \text{ \AA}$ , in good agreement with literature values  $a = 4.987 \text{ \AA}$  and  $c = 5.652 \text{ \AA}$  [PDF#04-0498].<sup>9</sup> The observed peak intensities are in good agreement with those of a randomly oriented powder sample.

To synthesize  $\text{GeO}_2$  nanocubes with a wide range of sizes, we have systematically been varying the concentration ratio between the water solution and CTAB,  $\omega = [\text{water solution}]/[\text{CTAB}]$ . It is found that the average size of  $\text{GeO}_2$  nanocubes increases from 50 to 520 nm when  $\omega$  increases from 4.0 to 28.3. At the same time, the size distribution of  $\text{GeO}_2$  nanocubes becomes wider as shown in Figure 3. XRD patterns for various values of  $\omega$  are shown in Figure 3e. The average size of the nanocubes, as estimated from the Scherrer equation, is consistent with the TEM observations.

The effects of several parameters have been systematically investigated: the pH value of the water solution, the choice of oil phase, and the concentration ratio  $\omega$ . Varying the pH value of the water solution leads to dramatic changes in the size and shape of the  $\text{GeO}_2$  particles as shown by the TEM images in Figure 4. At high pH values, the shape of the particles changes from cubic to spherical. At low pH values, regular cubes are formed. Cubic shapes are also obtained for hydrolysis of  $\text{GeCl}_4$  under acidic conditions (Figures 4a and 4b). Rhombs-, triangle-, and hexagon-shaped particles are formed at pH = 7.0 (Figure 4c). The particles agglomerate with an average size of about 83 nm (Figure 4d) and with an irregular shape at pH = 13.0. At pH > 9.0, the product becomes  $\text{H}_3\text{Ge}_2\text{O}_6^{2-}$  as observed by several authors.<sup>10</sup> Under strong alkalic conditions (using hydrazine hydrate as water solution), amorphous  $\text{GeO}_2$  is obtained.

Figure 5a shows XRD patterns for samples prepared at different pH values of the water solution. Infrared spectra

(9) Powder Diffraction File (PDF). International Centre for Diffraction Data (ICDD), Newtown Square, PA.

(10) (a) Kawai, T.; Usui, Y.; Kon-No, K. *Colloid Surf., A* **1999**, 149, 39–47. (b) Kanno, Y.; Nishino, J. *J. Mater. Sci. Lett.* **1993**, 12, 110–112.

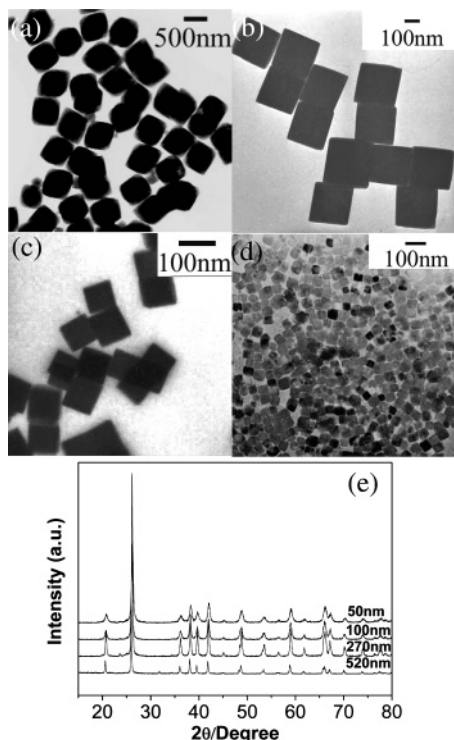


**Figure 3.** TEM and XRD patterns of GeO<sub>2</sub> nanocubes prepared by varying the concentration ratio  $\omega$ . (a–d) TEM images for GeO<sub>2</sub> cubes with average sizes of 494, 288, 105, and 67 nm corresponding to  $\omega = 28.3, 12.1, 8.1,$  and 4.0, respectively; (e) XRD patterns of GeO<sub>2</sub> cube samples in a–d, in which average particle sizes of 520, 270, 100, and 50 nm, respectively, were estimated from the line broadening of the 101 diffraction peak ( $2\theta = 26^\circ$ ) using the Scherrer equation.

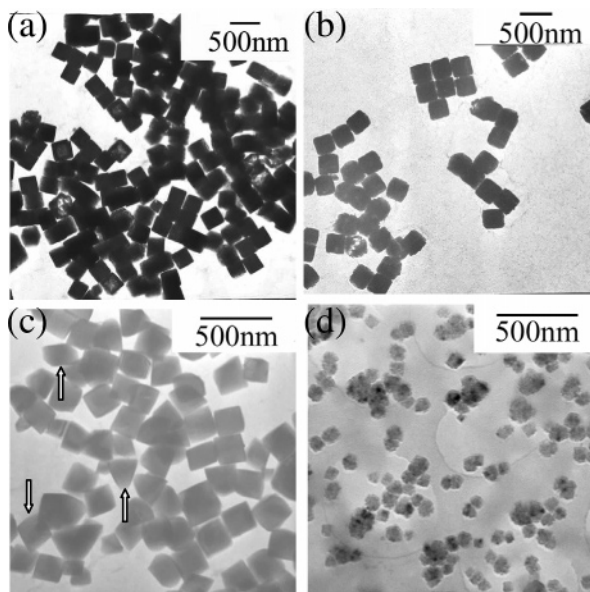


**Figure 4.** (a–d) TEM images of GeO<sub>2</sub> nanoparticles prepared with heptane as the oil phase at different pH values, 1.0, 3.0, 7.0, and 13.0, of the water solution. Arrows in c show rhombs-, triangle-, and hexagon-shaped particles.

(FTIR) were also recorded (Figure 5b). It is found that, after the washing procedure, no IR bands corresponding to organic species (e.g., C–H, C–C, C=O, N–H, C–N) were detected, indicating that little or no CTAB and oleylamine is present on the nanocubes. For  $\text{pH} \leq 9.0$ , four peaks of  $\alpha\text{-GeO}_2$  are detected at 516, 552, 585, and 882  $\text{cm}^{-1}$ . For  $\text{pH} > 9.0$ , only two peaks at 536 and 776  $\text{cm}^{-1}$  are assigned to the

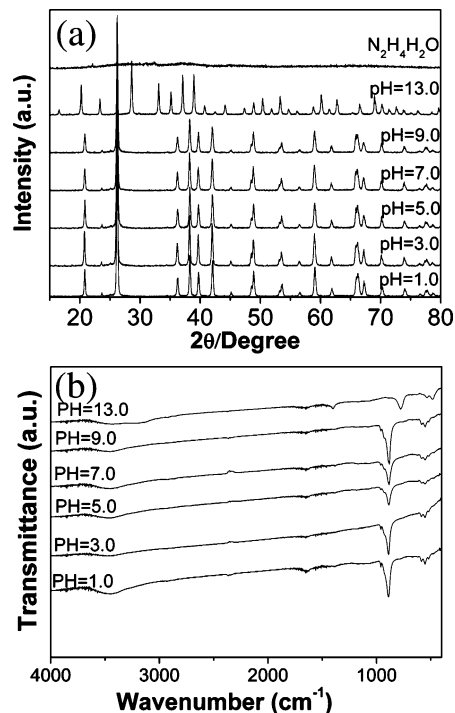
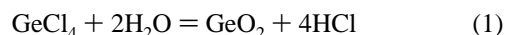


**Figure 5.** (a) XRD patterns of samples obtained at different pH values of the water solution. When the water solution is  $\text{N}_2\text{H}_4\text{H}_2\text{O}$ , the sample is amorphous. (b) FTIR patterns of samples obtained under different pH values of the water solution.

Ge–O stretching modes of the  $\text{H}_3\text{Ge}_2\text{O}_6^-$  phase, which is a precursor of GeO<sub>2</sub>.<sup>10</sup> The main reactions of hydrolysis of GeCl<sub>4</sub> in a water solution can be described as follows:



For  $\text{pH} < 9.0$ , the reversible reaction 1 may occur. This means that, at the beginning, the concentration of GeCl<sub>4</sub> is low. The reaction then proceeds toward the left. Nucleation of GeO<sub>2</sub> particles is difficult because the small nuclei formed initially are dissolved, owing to the high concentration of  $[\text{H}^+]$ . When  $[\text{GeCl}_4]$  increases, GeO<sub>2</sub> nuclei are formed through homogeneous nucleation. These nuclei may be wrapped by surfactant (CTAB and oleylamine) in micelles and grow into cubes. Reaction 2 occurs when the water solution is alkaline. For  $\text{pH} > 9.0$ , a few nuclei of the intermediate  $\text{H}_3\text{Ge}_2\text{O}_6^-$  phase can be wrapped by the surfactant in micelles as observed in Figure 4d.

To investigate the effect of the oil phase, we performed experiments using octane as the oil phase with various pH values, as shown in the Supporting Information (S1). At  $\text{pH} = 1.0$ , cube-shape particles are still formed. For increasing the pH values, capsule-shaped particles are detected (S1b and S1c) with a relatively uniform size. A large magnification image (the inset of S1b) of two capsules reveals that the capsules are hollow. At  $\text{pH} = 13.0$ , the shape of the particles becomes irregular, like the case where heptane is used as the oil phase (Figure 4d). The ratio between the concentrations of the water solution and the surfactant can modify the size of the micelle.

To understand the mechanism of formation of GeO<sub>2</sub> nanocubes under acid conditions, we have applied the classic

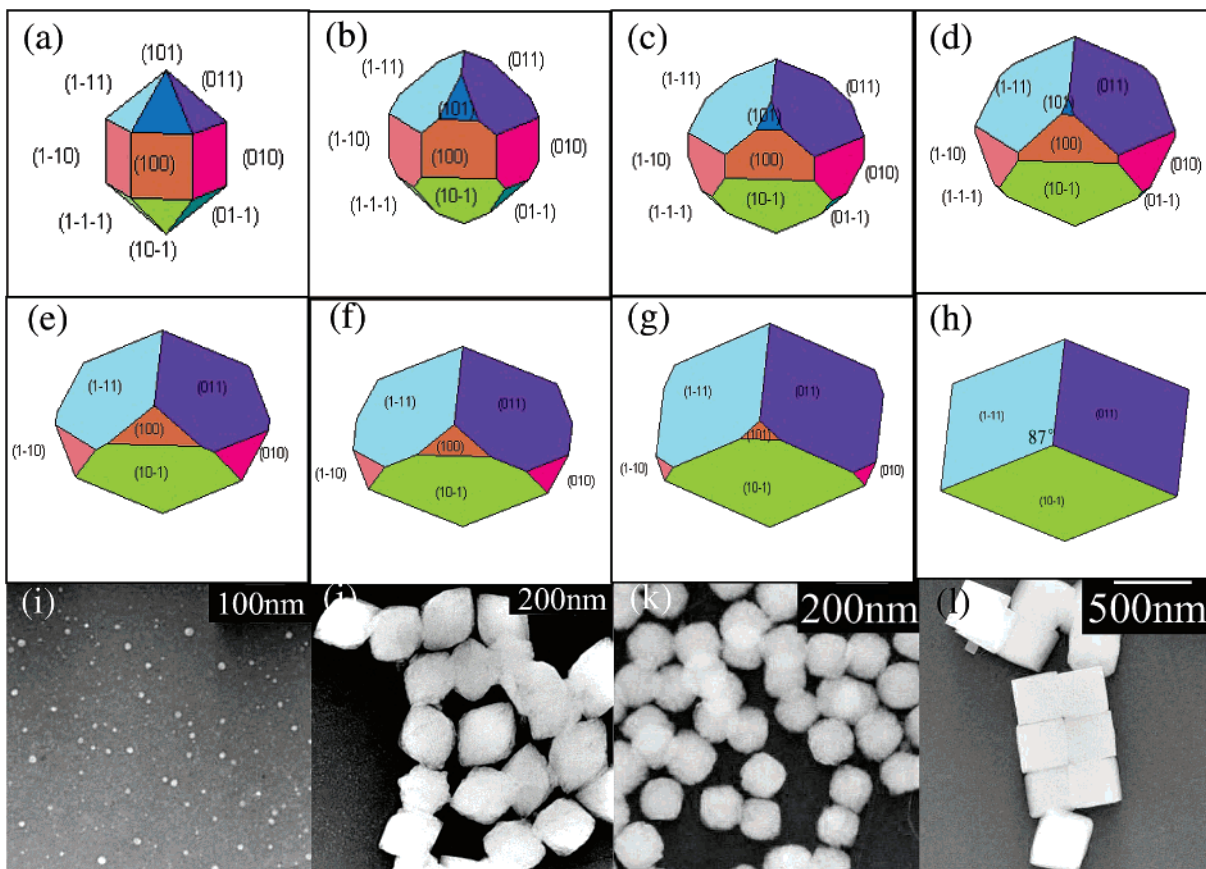


**Figure 6.** (a–h) Simulated geometries of GeO<sub>2</sub> particles during the growth process under acid conditions; (i–l) TEM images of GeO<sub>2</sub> samples obtained for 0.5, 1, 2, and 3 h reaction times. The pH value of the water solution is 1.0 with heptane as the oil phase.

BFDH method, as suggested by Bravais, Freidel, Donnary, and Harker, and the HP model, proposed by Hartman and Perdok.<sup>11</sup> The BFDH model assumes that the most energetically stable and slowest growing faces are the ones with the highest density of material and the largest spacing between adjacent layers. It suggests that the planes having a strong tangential force and a weak normal force are the most dominant faces. The growth velocity,  $R_{hkl}$ , along the normal direction of a crystal plane ( $hkl$ ) is inversely proportional to the interplanar spacing,  $d_{hkl}$ . Thus, the ideal shape of a particle of hexagonal GeO<sub>2</sub> consists of two hexagonal pyramids at the ends and a hexagonal prism in the middle, as illustrated in Figure 6a.

According to the HP model, the growth rate  $R_{hkl}$  depends on the attachment energy,  $E_{hkl}^{\text{att}}$ , of the ( $hkl$ ) plane. Using the Morphology Package of the Material Studio, attachment energies for various crystallographic planes of hexagonal GeO<sub>2</sub> have been calculated and listed in the Supporting Information (S2). The faces with low attachment energies are the most prominent faces during the crystal growth. Finally, the morphologic evolution of hexagonal GeO<sub>2</sub> under acid conditions has been determined, as shown in Figures 6a–h. It found that the hexagonal prism with two hexagonal pyramids at both ends slowly gets a truncated cubelike shape and finally a cubelike shape (with 87° between (011) and (10 $\bar{1}$ )), in perfect agreement with the present experimental observations (Figures 6i–l).

## Conclusions

In summary, monodisperse GeO<sub>2</sub> nanocubes with sizes ranging from 50 to 520 nm have been synthesized by hydrolysis of GeCl<sub>4</sub> in the presence of oleylamine and cetyltrimethylammonium (CTAB) in a reverse micelle method. The pH value of the water solution and the concentration of the surfactant strongly affect the size and shape of the GeO<sub>2</sub> nanoparticles produced. Due to the effect of H<sup>+</sup> etching, monodisperse GeO<sub>2</sub> cubelike particles with an angle of 87° between (011) and (10 $\bar{1}$ ) can be formed. The shape evolution of the GeO<sub>2</sub> nanocubes can be explained by the correlation of growth rate with attachment energy of different crystallographic planes using the BFDH and Hartman-Perdok (HP) models.

**Acknowledgment.** The authors would like to thank BSRF in Beijing, and NSRL in Hefei, P.R. China; HASYLAB in Hamburg, Germany; MAX-Lab in Lund, Sweden; KEK and SPring8 in Japan for use of the synchrotron radiation facilities. Financial support from the National Natural Science Foundation of China (Grants Nos. 50341032 and 50425102), the Ministry of Science and Technology of China (Grant Nos. 2004/249/37-14 and 2004/250/31-01A), the Ministry of Education of China (Grant Nos. 2.005E+10 and 2005-55), and Zhejiang University is gratefully acknowledged.

**Supporting Information Available:** S1: TEM images of GeO<sub>2</sub> with capsule shape using octane as the oil phase. S2: Calculated attachment energies of GeO<sub>2</sub>.